Structural characterization and low temperature growth of ferromagnetic Bi–Cu codoped ZnO bicrystal nanowires

C. Xu,[a] J. Chun, and D. Kim[b]
Physics Department and Electron Spin Science Center, POSTECH, San 31, Hyoja-Dong, Namku, Kyungbuk 790-784, Republic of Korea

B. Chon and T. Joo
Department of Chemistry, POSTECH, Pohang, 790-784, Republic of Korea

(Received 2 June 2007; accepted 10 September 2007; published online 8 October 2007)

Ferromagnetic Bi–Cu codoped ZnO nanowires were fabricated at temperatures as low as 300 °C via a vapor phase transport using the mixture of Zn, BiI_3 and CuI powders. They are grown as a bicrystal, along the $[01\bar{1}2]$ direction, have a width of 40–150 nm, and a length of a few microns. The investigation of the growth mechanism proposes that the synergy of BiCu and iodine/iodide induces the formation of bicrystallinity. The photoluminescence measurement shows the cooperative effect of Bi and Cu ions. The ferromagnetism observed in this study is the result of the combined effect of structural defects, the substitution of Cu into Zn site along the *c* axis, and codoping of Bi. © *2007 American Institute of Physics*. [DOI: 10.1063/1.2791005]

Studies on the ferromagnetism of dilute magnetic semiconductor film such as Mn–ZnO[1] and Co–ZnO[2] have been reported. However, the origin of room temperature (RT) ferromagnetism, whether it arises from intrinsic property or impurity phase, is still in debate. It is thought that the dopant itself can easyly form magnetic impurities such as Mn_3O_4, Co, and CoO. This contention prompts one to search for metals in which neither metal itself nor its compound is magnetic. Cu is well suited because itself and its oxides are nonmagnetic and can be a magnetic ion of +1/2 spin in the 2+ state. On the other hand, the low temperature fabrication of Cu doped ZnO single or bicrystal nanowires (NWs) enables one to integrate other processing techniques into nanodevices since high temperature (>400 °C) is not well suited to other processing techniques.[3] Acting as a catalyst, Bi is useful for low temperature fabrication of ZnO NWs due to its low melting point.[3] Although works on Cu doped ZnO film and bulk have been reported, the study on *in situ* ferromagnetic BiCu codoped ZnO bicrystal NWs grown at low temperatures is still lacking.

In this letter, we report *in situ* growth of Bi–Cu codoped ZnO bicrystal NWs at a temperature as low as 300 °C and the characterization of their magnetic and optical properties. Zinc (Zn, 99.998%, 100 mesh, Aldrich), bismuth iodide (BiI_3, 99.999%, Aldrich), and cuprous iodide (99.99%, Aldrich) with a weight ratio of 3:1:1 were mixed homogenously in a mortar and ground using a pestle for ~15 min. The mixture was loaded into an 8-cm-long alumina boat that was then covered by three pieces of oxidized silicon substrates/sapphire substrates with gaps of ~1 mm. The covered boat was subsequently placed in the center of a quartz tube. The base vacuum was about 300 mTorr. A high purity argon gas at a flow rate of 80 cubic centimeter per minute at STP was fed into the quartz tube. The furnace was heated to 300 °C and stayed at this temperature for 30 min along with momentary introduction of air into the reaction chamber via the outlet end of the furnace.

Figure 1 shows the scanning electron microscope (SEM) image of as-fabricated samples having a wire shape with a width of 40–150 nm and a length of up to a few microns. The SEM-based energy dispersive x-ray spectrometry (EDX) analysis shows that the bicrystal NW consists of Zn, O, Bi, and Cu. The transmission electron microscopy (TEM) image of a single bicrystal NW with grain boundary (GB) in the middle along the length is shown in Fig. 1(b). The NW has a width of about 50 nm. The selected area electron diffraction pattern [Fig. 1(c)] shows two sets of spots with the $[2\bar{1}\bar{1}0]$ zone axis of ZnO, which can be indexed as wurtzite hexagonal structure. No secondary phase was observed. EDX with copper-free TEM grid indicates that the nanowire consists of Zn, O, and Cu with atomic ratio of 48.3, 51.4, and 0.3. Cu

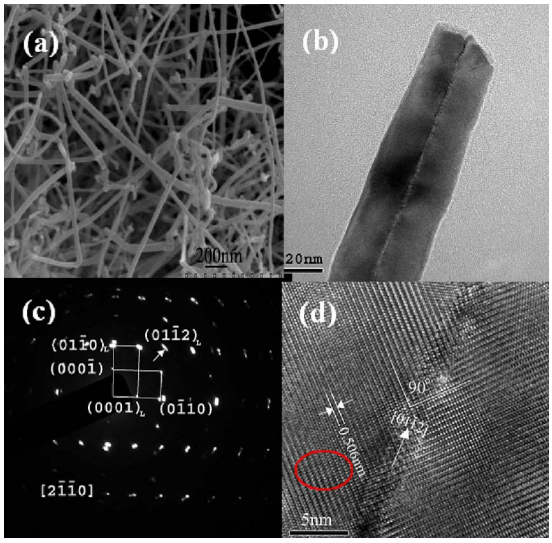

FIG. 1. (Color online) (a) SEM image of as-fabricated ZnO bicrystal NWs. (b) TEM image of a single bicrystal ZnO nanowire. (c) SAED pattern of the bicrystal NW. (d) HRTEM shows atomic lattices and lattice distortion indicated by the oval.

[a]Electronic mail: congkangxu@gmail.com
[b]Author to whom correspondence should be addressed. Electronic mail: kimd@postech.ac.kr

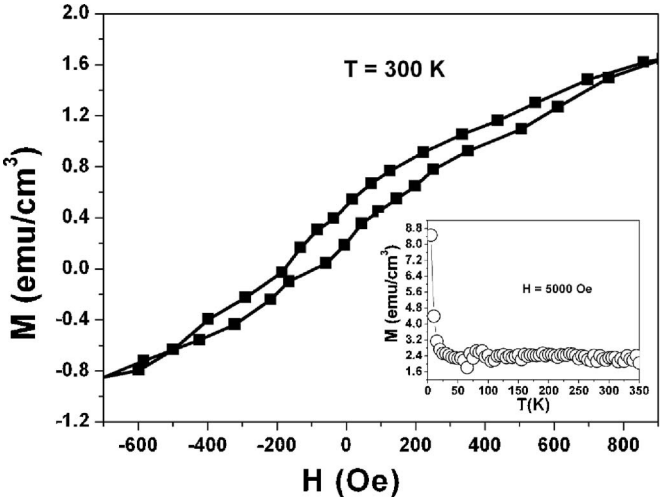

FIG. 2. RT *M-H* curve and *M-T* curve (inset) for Bi–Cu codoped ZnO bicrystal NWs on an oxidized Si substrate.

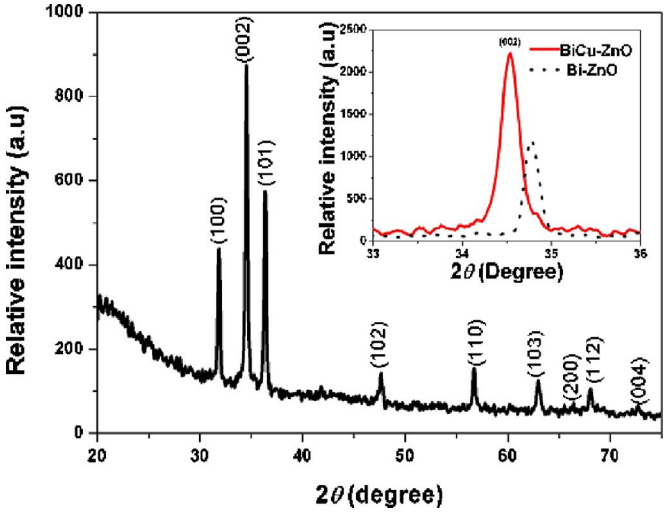

FIG. 3. (Color online) XRD pattern of bicrystal NWs. The inset is the (002) peaks from Bi–Cu bicrystal NWs and Bi–ZnO NWs. The (002) peak of bicrystal NWs has an angle shift of ~0.22° toward a lower angle as compared to Bi–ZnO NWs.

concentration is about 0.6 at. % and Bi being below detectable limit. The high-resolution (HR) TEM image [Fig. 1(d)] exhibits two sets of clear lattice fringes of the $[2\bar{1}\bar{1}0]$ zone axis. The angle between the (0001) planes in the two crystals is 90°. The bicrystal NW grows along the $[01\bar{1}2]$ direction perpendicular to the $[2\bar{1}\bar{1}0]$ zone axis. No secondary phase or clusters were observed, further verifying that Cu has been doped into ZnO lattice.

The magnetic properties of BiCu–ZnO nanostructures were investigated using a superconducting quantum interference device (SQUID) magnetometer. Figure 2 depicts the field dependences of magnetization (*M-H*) of the nanostructures on an oxidized Si substrate at room temperature. The contributions from the substrate have been subtracted. The hysteresis loop clearly indicates that the bicrystal NWs have a ferromagnetism with a remanence (M_r) of ~0.5 emu/cm^3. The inset is the *M-T* curve, a further indicative of ferromagnetism. The absence of a ferromagnetic transition in the *M-T* plot indicates T_c in excess of the 350 K temperature limit of the SQUID device. The observed ferromagnetism can be attributed to the structural defects such as GB and lattice distortion, as shown in Fig. 1. The fact that ferromagnetism can be developed due to the structural defects has been observed experimentally in Cu–ZnO film,[4] Cr–TiO_2 films,[5] Ni–ZnO nanocrystals,[6] as well as can be explained theoretically by the bound magnetic polaron mechanism[7] and donor-impurity exchange model.[8]

The x-ray diffraction pattern of bicrystal NWs is shown in Fig. 3. The major diffraction peaks can be indexed as the hexagonal wurtzite structure ZnO.[9] Although the radius of Cu^{2+} ion (0.057 nm) is slightly smaller than the Zn^{2+} ion (0.06 nm), the position of the dominant peak (002) of BiCu–ZnO bicrystal NWs is shifted toward the lower angle rather than the higher angle with respect to Bi–ZnO NWs (inset)[3]. The angle is shifted by 0.12°, which corresponds to the increase of the lattice spacing by 0.70%. A similar observation has been also made in Cu doped ZnO film[4] and Co doped ZnO[10] where the radius of the Co^{2+} (0.058 nm) is smaller than the Zn^{2+}. The fact that the dominant peak is (002) in our sample and the peak is shifted as Cu is doped indicates that Cu is substituted into Zn sites along the *c* axis. This could also contribute to the observed ferromagnetism as the theoretical study by Feng showed that the substitution of Cu into Zn sites along the [0001] direction leads to ferromagnetism.[11]

Figure 4 shows the photoluminescence (PL) spectra recorded at 10 K (a) and 300 K (c) of bicrystal BiCu–ZnO NWs excited by 355 nm light. For comparison, the room temperature PL spectra [Fig. 4(b)] of single crystal Bi–ZnO NWs is shown.[3,12] At 10 K, only two distinct peaks of ultraviolet emission (UV) peak at 369 nm and the green emission (GE) centered at 500 nm appears. All other often-observed peaks in the UV region at low temperatures have been screened. At 300 K, the UV is shifted to 381 nm and GE to 502 nm. For ZnO, the UV generally originates from the radiative recombination (RR) of excitons,[13] and the GE from the RR of a photo-generated hole with an electron occupying the singly ionized oxygen vacancy in ZnO.[14] From low temperature to room temperature, the redshift and broadening of peaks can be attributed to phonon scattering. Compared with the room temperature PL spectra of Bi–ZnO NWs (UV at 395 nm, GE at 512 nm), the UV and GE of bicrystal NWs have a blueshift of 14 and 10 nm, respectively. Since the diameters of bicrystal ZnO NWs (~50 nm) and Bi–ZnO NWs (~40 nm) are not comparable to excitonic Bohr radius (~2.4 nm) of bulk ZnO, the quantum confinement effect is

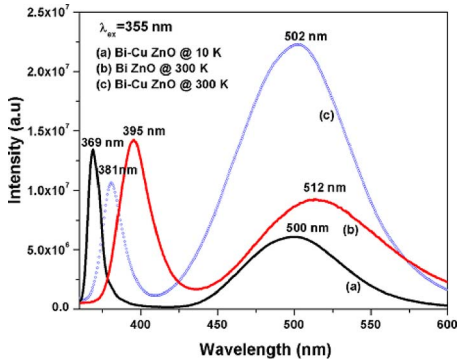

FIG. 4. (Color online) PL spectra of bicrystal BiCu–ZnO NWs at 10 K (a) and 300 K (c) as well as single crystal Bi–ZnO NWs at 300 K (b). The wavelength of the excitation source is 355 nm.

not responsible for the blueshifts. On the other hand, the reported spectra of ZnO:Cu bulk crystals and NWs usually show a GE ranging from 430 to 650 nm which was redshifted with increasing Cu dopants.[15,16] Compared with undoped ZnO NWS (UV at 386 nm, GE at 520 nm),[16] the UV of Bi doped ZnO NWs has also a redshift of 9 nm, whereas the GE has a blueshift of 8 nm. The observed blueshift of the GE could not be related to Cu^{+} which causes the redshift of ZnO GE. Two possibilities then remain: one is the effect by Bi dopants, i.e., the localized excitation ($^1S_0 \rightarrow {}^3P_1$) of Bi^{3+}, as reported in Bi-doped ZnO hierarchical nanostructures,[17] and the other is the effect by Cu^{2+} dopants. The blueshift of the UV can be tentatively assigned to the cooperative effect of codoping of Bi and Cu since separate Bi or Cu dopant by and large leads to redshift rather than blueshift.[16,17] These results therefore show the interplay of Bi and Cu for ZnO, and that Bi and Cu have been doped into ZnO. The doping of Bi into ZnO would lead to electron doping. This could also make a contribution to the observed ferromagnetism since the donor-impurity exchange model[8] by Coey *et al.* suggests that *n*-type conduction is helpful for the development of ferromagnetism.

Several supporting experiments were carried out to clarify the growth mechanism of ferromagnetic bicrystal nanowires. The results indicate that (a) no bicrystal nanowire is obtained at temperatures of 250–300 °C without CuI from the starting material and (b) no nanostructure is obtained below 350 °C without BiI_3 from the starting material. (c) No bicrystal nanowires but large diameter single crystal nanowires/nanorods are obtained in the case of the substitution of Bi and Cu for BiI_3 and CuI. The growth of ZnO bicrystal nanowires may be proposed as follows: Zn–Bi droplets are initially formed around 250 °C, similar to Bi–ZnO nanowires at a low temperature.[14] The newly formed droplets are carried away and then deposited on the substrate. As the temperature rises, Zn–Bi droplets absorb Cu arising from the sublimation of CuI and subsequently form Zn–Bi–Cu liquid droplets, analogous to Zn–Bi–Mn droplets.[18] Only in the case of Bi–Cu can the bicrystal nanowires be obtained. Hence, we suggest that Bi–Cu plays an important role on the formation of bicrystal nanowires. ZnO starts to nucleate as air is intentionally introduced into the furnace. Since ZnO is not soluble in the liquid phase, ZnO would precipitate from Zn–Bi–Cu droplets; concurrently, Bi–Cu would be incorporated into the ZnO to form ZnO twinlike nucleus since Bi can easily induce GB in Cu,[19,20] leading to a bicrystal nanowire with a preferential growth along the $[01\bar{1}2]$ direction. The preference of the ZnO bicrystal nanowires to grow in the $[01\bar{1}2]$ direction is probably associated with I^{-} and I_2 as previously reported.[12] ZnO can be concisely depicted as a number of alternating planes, consisting of tetrahedrally coordinated O^{2-} and Zn^{2+} ions, stacked alternately along the *c* axis. The oppositely charged ions result in a spontaneous polarization along the *c* axis as well as divergence in surface energies.[21] Because I^{-} and I_2 are highly polarizable,[22] the sublimation of iodide and/or iodine facilitates iodine anions and/or iodine molecules to interact with the polar ZnO surface and change the surface energies, leading to bicrystal nanostructures with GBs. The growth of ferromagnetic ZnO bicrystal nanowires is therefore dominated by the synergy of vapor-liquid-solid and the polarization of iodide or iodine. Based on the growth mechanism and structural characterization, BiCu facilitates the formation of bicrystal NWs with GBs and lattice distortions. These structural defects contribute to the activation of ferromagnetism as demonstrated both experimentally and theoretically. 0

This work was supported in part by electron Spin Science Center (eSSC) and in part by National Research Laboratory Program funded by Korean Science and Engineering Foundation (KOSEF).

[1] P. Sharma, A. Gupta, K. V. Rao, F. J. Owens, R. Sharma, R. Ahuja, J. M. O. Guillen, B. Johansson, and G. A. Gehring, Nat. Mater. **2**, 673 (2003).
[2] S. Ramachandran, A. Tiwari, and J. Narayan, Appl. Phys. Lett. **84**, 5255 (2004).
[3] C. K. Xu, K. Rho, J. Chun, and D. E. Kim, Appl. Phys. Lett. **87**, 253104 (2005).
[4] T. S. Herng, S. P. Lau, S. F. Lau, S. F. Yu, H. Y. Yang, X. H. Ji, J. S. Chen, N. Yasui, and H. Inaba, J. Appl. Phys. **99**, 086101 (2006).
[5] T. C. Kaspar, S. M. Heald, C. M. Wang, J. D. Bryan, T. Droubay, V. Shutthanandan, S. Thevuthasan, D. E. McCready, A. J. Kellock, D. R. Gamelin, and S. A. Chambers, Phys. Rev. Lett. **95**, 217203 (2005).
[6] P. V. Radovanovic and D. R. Gamelin, Phys. Rev. Lett. **91**, 157202 (2003).
[7] R. N. Bahtt, M. Berciu, M. P. Kennet, and X. Wan, J. Super.: Inc. **15**, 71 (2002).
[8] J. M. D. Coey, M. Venkatesan, and C. B. Fitzgerald, Nat. Mater. **4**, 173 (2005).
[9] JCPDS Card No. 36-1451 Plenum Publishing Corporation.
[10] S. Kolesnik, B. Dabrowski, and J. Mais, J. Appl. Phys. **95**, 2582 (2004).
[11] X. Feng, J. Phys.: Condens. Matter **16**, 4251 (2004).
[12] C. K. Xu, D. E. Kim, J. Chun, K. Rho, B. Chon, S. Hong, and T. Joo, J. Phys. Chem. B **110**, 2174 (2006).
[13] J. J. Wu, H. I. Wen, C. H. Tseng, and S. C. Liu, Adv. Funct. Mater. **14**, 806 (2004).
[14] Y. C. Kong, D. P. Yu, B. Zhang, W. Fang, and S. Q. Feng, Appl. Phys. Lett. **78**, 407 (2001).
[15] S. Zhou, X. Zhang, X. Meng, K. Zou, X. Fan, S. Wu, and S. Lee, Nanotechnology **15**, 1152 (2004).
[16] N. Y. Garces, L. Wang, L. Bai, N. C. Giles, and L. E. Halliburton, Appl. Phys. Lett. **81**, 622 (2002).
[17] C. K. Xu, K. Rho, J. Chun, and D. Kim, Nanotechnology **17**, 60 (2006).
[18] C. K. Xu, J. Chun, K. Rho, H. Lee, Y. Jeong, and D. E. Kim, Appl. Phys. Lett. **89**, 093117 (2006).
[19] G. Buscher, M. F. Chisholm, U. Alber, and M. Ruhle, Nat. Mater. **3**, 621 (2004).
[20] A. M. Donald and L. M. Brown, Acta Metall. **27**, 59 (1979).
[21] Z. L. Wang, X. Y. Kong, Y. Ding, P. Gao, W. Hughes, R. Yang, and Y. Zhang, Adv. Funct. Mater. **14**, 904 (2004).
[22] Y. Song, Y. Niu, H. Hou, and Y. Zhu, J. Mol. Struct. **689**, 69 (2004).